AHEAD OF PRINT

Icariin ameliorates osteoporosis by activating autophagy in ovariectomized rats

Jiaying Zou[B–D], Yue Peng[B], Yue Wang[B], Shouzhu Xu[C], Chuandao Shi[A], Qiling Liu[E,F]

Department of Epidemic and Health Statistics, College of Public Health, Shaanxi University of Chinese Medicine, Xianyang, China

A – research concept and design; B – collection and/or assembly of data; C – data analysis and interpretation;
D – writing the article; E – critical revision of the article; F – final approval of the article

Advances in Clinical and Experimental Medicine, ISSN 1899–5276 (print), ISSN 2451–2680 (online) *Adv Clin Exp Med*. 2024

Address for correspondence
Qiling Liu
E-mail: liuqilingsan@163.com

Funding sources
This study was funded by Qinchuangyuan Traditional Chinese Medicine Innovation Research and Development Transformation Project of Shaanxi Provincial Administration of Traditional Chinese Medicine (grant No. 2022-QCYZH-007), Shaanxi Provincial Administration of Traditional Chinese Medicine Program (grant No. 2021-ZZ-JC005) and the Shaanxi Provincial Key Research and Development Program (grants No. 2021SF-275, 2022SF-357).

Conflict of interest
None declared

Received on April 10, 2023
Reviewed on April 24, 2023
Accepted on October 12, 2023

Published online on January 18, 2024

Abstract

Background. Osteoporosis (OP) is a major problem that increases the mortality and disability rate worldwide. With an increase in the aging population, OP has become a major public threat to human health. Searching for effective and suitable targets for drug treatment in OP has become an urgent need.

Objectives. Osteoporosis is a metabolic bone disease characterized by reduced bone mass and density as well as micro-architectural deterioration. Icariin is a flavonoid extracted from plants of the genus *Epimedium* and has been shown to exert potential anti-OP activity. The present study was designed to observe the effect of icariin on OP and to clarify the underlying mechanisms in ovariectomized (OVX) rats.

Materials and methods. Hematoxylin and eosin (H&E) staining, von Kossa staining and micro-computed tomography (micro-CT) confirmed significant bone loss in the OVX group. Protein expression level was detected with western blot analysis.

Results. Icariin reversed a trend of increased bone turnover by reducing serum alkaline phosphatase (ALP), procollagen type I N-terminal propeptide (PINP), tartrate-resistant acid phosphatase isoform 5b (TRACP-5b), and C-telopeptide of type I collagen (CTX-I). Furthermore, icariin decreased sequestosome 1 (p62) and increased microtubule-associated protein 1 light chain 3II/microtubule-associated protein 1 light chain 3I (LC3II/LC3I), autophagy-related protein 7 (Atg7), and Beclin 1 in the femur of OVX rats, improving the indicators of impaired autophagy in OP.

Conclusions. Icariin reversed the significant upregulation of the serine/threonine protein kinase (Akt), mammalian target of rapamycin (mTOR) and unc-51-like autophagy activating kinase 1 (ULK1) at Ser757, and the downregulation of p-AMP-activated protein kinase (p-AMPK) and ULK1 phosphorylated at Ser555 in the OVX rats, suggesting that the mechanism of icariin action in OP treatment involves the activation and suppression of the AMPK/ULK1 and AKT/mTOR/ULK1 autophagy pathways, respectively.

Key words: autophagy, icariin, osteoporosis, AMP-activated protein kinase/Unc-51-like autophagy activating kinase 1, serine/threonine protein kinase/mammalian target of rapamycin/Unc-51-like autophagy activating kinase 1

Cite as
Zou J, Peng Y, Wang Y, Xu S, Shi C, Liu Q. Icariin ameliorates osteoporosis by activating autophagy in ovariectomized rats [published online as ahead of print on January 18, 2024]. *Adv Clin Exp Med*. 2024. doi:10.17219/acem/174078

DOI
10.17219/acem/174078

Background

Osteoporosis (OP) is a common degenerative bone disease characterized by a reduction in bone mass and the degradation of micro-architectural structures.[1] Epidemiological surveys show that over 200 million women are affected by OP globally, with 8.9 million fractures each year. According to the latest projections, the prevalence of OP will reach 13.6 million by 2030 in women aged ≥50 years.[2] Osteoporosis has become the leading cause of disability and death in the elderly population.

Many phytochemicals are good substitutes for chemically synthesized medications for the treatment of various human diseases.[3] Icariin, the main flavonoid isolated from the plant of the genus *Epimedium*, has been identified as a potential drug for treating OP.[4–6] Icariin mainly affects bone metabolism and promotes bone resorption by regulating estrogen, skeletal accretion, as well as apoptosis and its related signaling pathways. The common signaling pathways include PI3K-Akt, Wnt/β-catenin, and RANKL/RANK/OPG. They are essential for restoring the balance between bone resorption and formation in the bone remodeling process.[7]

Autophagy is critical for maintaining bone homeostasis through the degradation of abnormal proteins and pathogenic microorganisms. Research links low autophagy to OP.[8–11] Osteoblasts (OBs) and osteoclasts (OCs) play a crucial role in maintaining bone homeostasis, and the regulation of this process involves autophagy; when autophagy is deficient, it disrupts bone homeostasis and leads to OP.[12,13] However, the mechanisms mediating OP autophagy remain unclear.

Objectives

In our research, an OP model was established by ovariectomy in rats and icariin was administered by irrigation to study its effects and potential mechanism in autophagy and improvement of OP.

Materials and methods

Animals

The study was approved by the Animal Ethics Committee of the Shaanxi University of Chinese Medicine (approval No. SCXK (Shaanxi) 2019-001). Thirty female adult Sprague–Dawley (SD) rats (200–250 g), 3–4 months of age, purchased from the Experimental Animal Center of the Air Force Medical University (Xi'an, China), had access to clean water and food during the experiment, and were housed at 25°C with 50 ±10% humidity and a 12 h/12 h light-dark cycle.

In the present investigation, animal feed was purchased from Chengdu Dashuo Biological Technology Co., Ltd. (Sichuan, China), and its composition was the same in all experimental rats.

Experimental agents

Icariin (20200719) was purchased from Xi'an Yuhui Biotechnology Co. Ltd (Xi'an, China). Alkaline phosphatase (ALP) (JL26470), procollagen type I N-terminal propeptide (PINP) (JL49448), tartrate-resistant acid phosphatase isoform 5b (TRACP-5b) (JL12318), and C-telopeptide of type I collagen (CTX-I) (JL20748) enzyme-linked immunosorbent assay (ELISA) kits were purchased from Jianglai (Shanghai, China). Autophagy-related protein 7 (Atg7) (8558), Akt (9272), p-Akt (4058), Beclin1 (3495), mammalian target of rapamycin (mTOR) (2972), p-unc-51-like autophagy activating kinase 1 (ULK1) (Ser555) (5869), p-mTOR (2971), ULK1 (8054), p-ULK1 (Ser757) (14202), and AMP-activated protein kinase (AMPK) (5832) were purchased from Cell Signaling Technology (Danvers, USA). Microtubule-associated protein 1 light chain 3 (LC3) (GTX127375) was purchased from Genetex (Louis Park, USA), sequestosome 1 (p62) (ab109012) from Abcam (Cambridge, UK), β-actin (bs-0061R) from Bioss (Woburn, USA) and p-AMPK (13S4010) from Bioword (Louis Park, USA). Bicinchoninic acid (BCA) kits were purchased from Thermo Fisher Scientific (Waltham, USA) and dithiothreitol (DTT; 1 mol/L) was obtained from Sigma-Aldrich (St. Louis, USA).

Instruments

Mini-PROTEAN Tetra electrophoresis and blots, a protein semi-dry transfer device, and a gel imaging system were used (Bio-Rad, Hercules, USA). A full wavelength microplate reader (Tecan, Zurich, Switzerland), an automatic high-speed refrigerated centrifuge (Sigma-Aldrich), a SCIENTZ-48 Tissue Grinder (Xinzhi, Hunan, China), an X-Ray Micro-CT SkyScan 1276 (Bruker, Billerica, USA), and a VS200 digital slide scanner (Olympus, Tokyo, Japan) were utilized for tissue analysis.

Groups and animal treatments

Thirty female adult SD rats were randomly divided into control (sham-operated+saline, n = 10), model (ovariectomy+saline, n = 10) and icariin (ovariectomy+icariin, n = 10) groups. The model and icariin groups were subjected to bilateral ovariectomy, and the same amount of fat tissue near the ovary was removed in the control group. One week after the operation, intragastric administration of saline (0.5 mL/100 g) was carried out for 12 consecutive weeks in the model group, to which icariin (120 mg/kg) was added in the icariin group. Body weight of the animals was measured 14 times per week.

Rats were intraperitoneally anesthetized with 10% chloral hydrate (300 mg/kg), and, under anesthesia, blood was collected from the abdominal aorta until the blood flow was exhausted. Death was confirmed by cardiac and respiratory arrest. Bones were frozen to –80°C for testing. None of the rats had peritonitis or its associated symptoms after the administration of 10% chloral hydrate. Rats weighed 340–403 g, and less than 10 mL of blood was collected from each rat at the time of sacrifice.

Measurement of serum metabolism indexes

Serum PINP, ALP, CTX-I, and TRACP-5b are indicators for evaluating bone formation and resorption ability. The levels of ALP (JL26470), PINP (JL49448), TRACP-5b (JL12318), and CTX-I (JL20748) were detected with ELISA. Blood samples were stored at room temperature for 2 h, centrifuged at 4°C for 5 min (3000 rpm), and the serum was separated. The samples were prepared according to the index instruction, a standard curve based on the standard solutions was created, and the sample (50 µL) and horseradish peroxidase (HRP; 100 µL) were added to each well. The well was sealed and placed in a 37°C incubator, and after 60 min, the liquid was poured off, and the sample dried on the absorbent paper. The washing solution (350 µL) was added to each well and maintained for 1 min at room temperature; after repeating 5 times, reaction substrate solutions A (50 µL) and B (50 µL) were added to each well, and they were incubated for 15 min in a 37°C incubator. The termination solution (50 µL) was added to each well for 15 min. A regression equation was formulated according to the standard curve, and the sample optical density (OD) value (λ = 450 nm) was taken into the equation to calculate the sample concentration. The sample size was 7.

Measurement of bone morphology

Hematoxylin and eosin (H&E) staining was used to evaluate the morphological features of the femur. Right distal femurs (1-cm specimens) were fixed for 48 h with 4% paraformaldehyde, decalcified with 10% ethylenediaminetetraacetic acid (EDTA), embedded in paraffin, and sectioned (5-µm thickness). Sections were stained with H&E prior to digital slide scanning. The H&E staining was performed according to the reference literature.[14]

Detection of calcium nodules

Calcification nodules can reflect the level of the OB mineralization. Calcium nodules were observed using Von Kossa staining. Right distal femurs (1 cm specimens) were fixed for 48 h with 4% paraformaldehyde, embedded with paraffin, sectioned, and washed subsequently with xylene, gradient alcohol and distilled water. In the next step, 3% silver nitrate was added for 1 h and washed with water for 5 min, counterstain with toluidine blue for 5 min, then washed with distilled water repeatedly, dried, and sealed with neutral glue. The sample size was 3.

Micro-computed tomography

A micro-computed tomography (micro-CT) system was employed for trabecular bone mass measurement. At the time of execution, the left femur, tibia and vertebrae (L4) were separated and fixed for 24 h in 4% paraformaldehyde before flushing with 70% ethanol. Distal femoral and proximal tibia metaphysis were scanned at a resolution of 8 µm (80-kV voltage, 80-µA current). Micview V2.1.2 software (GE Healthcare, Chicago, USA) was used to analyze the data. Regions of interest segmented with a fixed threshold were reconstructed into 3-dimensional images. Trabecular bone was quantified using bone marrow density (BMD), bone volume over total volume (BV/TV), bone surface over bone volume (Bs/Bv), trabecular thickness (Tb.Th), trabecular number (Tb.N), and trabecular spacing (Tb.Sp). The sample size was 4.

Western blot analysis

Femur (500 mg) at –80°C was cut into fragments with bone shears, ground into powder in liquid nitrogen, and collected in a centrifugal tube. Samples were lysed using 700-µL radioimmunoprecipitation assay (RIPA) buffer and ground with a high-throughput grinder. The homogenized tissues were centrifuged (14,000 rpm, 20 min) at 4°C. The supernatant was transferred to a new EP tube, and 10 µL was separated for quantitative analysis using a BCA protein assay kit. The remaining part was treated with RIPA, ×2 loading buffer, and 1 M DTT by volume, heated for 8 min at 100°C, cooled, mixed and frozen at –80°C. Proteins (80 µg/well) were separated on a 10–15% sodium dodecyl sulfate polyacrylamide gel(SDS-PAGE). Separated proteins were subjected to electroblotting on polyvinylidene fluoride (PVDF) membranes. The membranes were then blocked and incubated with designated primary antibodies (rabbit anti-rat) overnight at 4°C (all antibodies were diluted). Using β-actin (1:5000) as internal control, the autophagy proteins Atg7 (1:2000), p62 (1:2000), LC3 (1:2000), Beclin1 (1:2000), Akt (1:1000), p-Akt (1:1000), mTOR (1:1000), p-mTOR (1:1000), p-AMPK (1:1000), ULK1 (1:1000), p-ULK1 (Ser555) (1:1000), and p-ULK1 (Ser757) (1:1000) were detected. On the following day, samples were washed 3 times (5 min/time) with Tris-buffered saline with Tween (TBST) and were incubated with goat anti-rabbit IgG conjugated to HRP for 2 h, and then the PVDF membranes were washed 4 times (5 min/time) with TBST. Finally, the membranes were exposed using a Molecular Imager® ChemiDoc™ XRS System, and the western blot data were analyzed using ImageJ software (National Institutes of Health (NIH), Bethesda, USA). The sample size was 3 for the western blot.

Statistical analyses

The analysis was carried out using IBM SPSS Statistics for Windows, v. 26.0 (IBM Corp., Armonk, USA). Data are presented as mean ± standard deviation (M ±SD). A normality test and homogeneity of variance test were first used for multiple group data; one-way analysis of variance (ANOVA) was used if the data were in accordance with normality and homogeneity of variance; otherwise, the Kruskal–Wallis H test was conducted. A normality test, homogeneity of variance test, sphericity test, and repeated measures analysis of variance test were used for repeated measure data. Fisher's least significant difference (LSD) or Dunn's post hoc test were performed if differences were significant. Differences were considered of statistical significance with $p < 0.05$.

Results

Body weight and condition of the OP rats were ameliorated by icariin

Body weight values increased in all groups after 12 weeks, with a significant uptrend in the model group compared to the control and icariin groups from the 2nd week. Icariin appeared to control body weight but not at a statistically different level when compared to the model group. The fur of the rats in the model group was drier, yellower and duller than that of the control group; reflexes were also slower. Compared to the model group, the icariin group rats exhibited more sleek and white fur, faster reaction times, and reduced body weight (Fig. 1 and Table 1).

Bone metabolism indexes of OP rats were mediated by icariin

The PINP, ALP, CTX-I, and TRACP-5b are indicators of bone metabolism, reflecting bone formation and resorption ability. In the model group, the expression of PINP, ALP, CTX-I, and TRACP-5b was increased. The 4 indexes were reduced in the icariin group compared with the model group (Fig. 2 and Table 2).

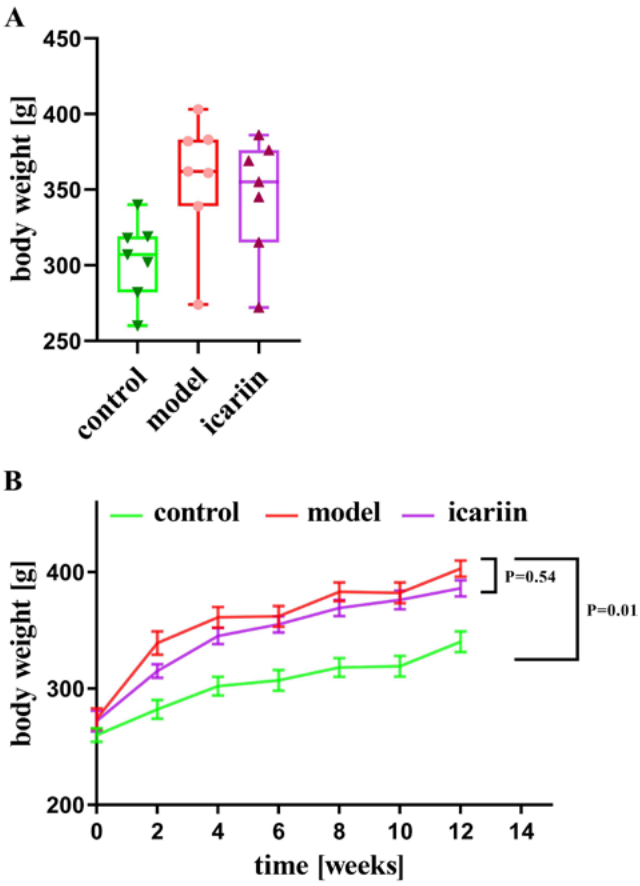

Fig. 1. Icariin ameliorated weight changes in osteoporosis (OP) rats. A. Box plots of 3 body weights at 12th week. Box bodies represent M (p_{25}, p_{75}), and upper bars and lower bars represent maximum and minimum, respectively (n = 7); B. The trend plots of body weight change in the 12 weeks ($F_{2,18} = 4.10$, $p = 0.03$). Repeated measures analysis of variance (ANOVA) and LSD post hoc tests were performed. Body weights in the model group increased form the 2nd week. Icariin could control body weights

Femoral morphological changes and calcium nodules in OP rats were restored by icariin

Morphological features of the femur were evaluated using H&E staining. Compared with the control group, the model group had more pathological changes, such as less femoral trabecular bone, uneven thickness, greater distance, and increased breakpoints. However, compared with the model group, the icariin group displayed multitudinous bone trabecula, and the bone microstructure was generally clear (Fig. 3A).

Table 1. Body weights (X ±S) of the rats at week 12

Group	Weight [g]	95% CI	F value (repeated measures ANOVA)	p-value
Control	340.00 ±9.00	279.68–328.32	4.10	0.03
Model	403.00 ±7.00*	318.72–396.71		
Icariin	386.00 ±7.00*	308.54–382.32		

* $p < 0.05$ compared to the control group; 95% CI – 95% confidence interval; ANOVA – analysis of variance.

Table 2. Expression of bone formation and resorption indexes in serum (X ±S)

Index	Group	Value [ng/mL]	95% CI	F value (one-way ANOVA)	p-value
PINP	control	1.42 ±0.59	0.87–1.97	24.84	0.00
	model	3.28 ±0.44***	2.88–3.69		
	icariin	2.44 ±0.44***##	2.03–2.85		
ALP	control	3.46 ±0.33	3.15–3.76	11.32	0.00
	model	5.01 ±0.66***	4.40–5.62		
	icariin	4.23 ±0.76*#	3.52–4.93		
CTX-I	control	1.16 ±0.18	0.99–1.32	33.61	0.00
	model	2.41 ±0.30***	2.13–2.69		
	icariin	1.84 ±0.35***###	1.51–2.16		
TRACP-5b	control	0.64 ±0.31	0.35–0.92	33.61	0.00
	model	1.86 ±0.34***	1.54–2.18		
	icariin	1.56 ±0.20***	1.38–1.75		

* $p < 0.05$ compared to the control group; *** $p \leq 0.001$ compared to the control group; #$p < 0.05$ compared to the model group; ##$p \leq 0.01$ compared to the model group; ###$p \leq 0.001$ compared to the model group; ALP – alkaline phosphatase; PINP – procollagen type I N-terminal propeptide; TRACP-5b – tartrate-resistant acid phosphatase isoform 5b; CTX-I – C-telopeptide of type I collagen; 95% CI – 95% confidence interval; ANOVA – analysis of variance.

The number of femoral calcium nodules was determined with von Kossa staining (Fig. 3B). There was a reduction in the number of calcium nodules in the model group. Compared with the model group, the icariin group displayed an increased trend in calcium nodules, but they were not significantly different (Fig. 3C, Table 3).

Table 3. Levels of calcium nodules in the femur (M (p_{25}, p_{75}))

Group	Gray value	H value	p-value
Control	119.52 (118.50, 120.60)	6.25	0.04
Model	29.39 (25.80, 31.40)*		
Icariin	52.45 (48.00, 53.80)		

*$p < 0.05$ compared to the control group.

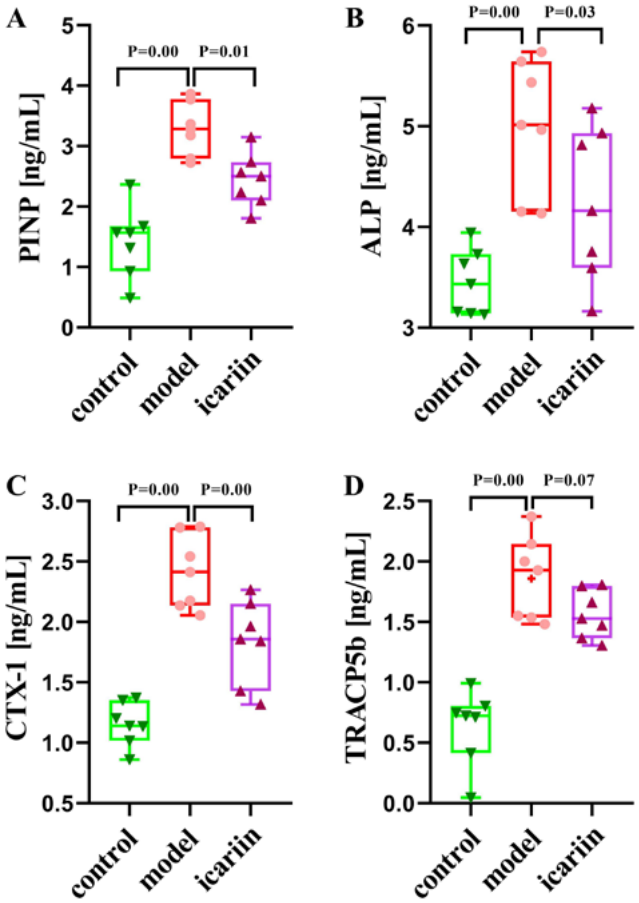

The BMD and trabecula state in OP rats was altered by icariin

The trabecular bone of the femur, tibia and lumbar spine (L4) were scanned with micro-CT (Fig. 4), revealing bone loss and atrophy of the bone trabecula in the model group and an improvement of the trabecular morphology and volume in the icariin group. Bone marrow density in the model group was lower than in the control group, while icariin increased the BMD compared with the model group.

Fig. 2. Icariin improved the bone formation and resorption indexes in serum shown using enzyme-linked immunosorbent assay (ELISA). A. The levels of procollagen type I N-terminal propeptide (PINP) in the serum of 3 groups ($F_{2,18} = 24.84$, $p = 0.00$); B. The levels of alkaline phosphatase (ALP) in the serum of 3 groups ($F_{2,18} = 11.32$, $p = 0.00$); C. The levels of C-telopeptide of type I collagen (CTX-I) in the serum of 3 groups ($F_{2,18} = 33.61$, $p = 0.00$); D. The levels of tartrate-resistant acid phosphatase isoform 5b (TRACP-5b) in the serum of 3 groups ($F_{2,18} = 33.61$, $p = 0.00$). One-way analysis of variance (ANOVA) and least significant difference (LSD) post hoc tests were performed in the A, B, C, and D plots. Box bodies represent M (p_{25}, p_{75}), and upper bars and lower bars represent maximum and minimum, respectively (n = 7). In the model group, the expression of PINP (A), ALP (B), CTX-I (C), and TRACP-5b (D) were increased, but icariin reduced them

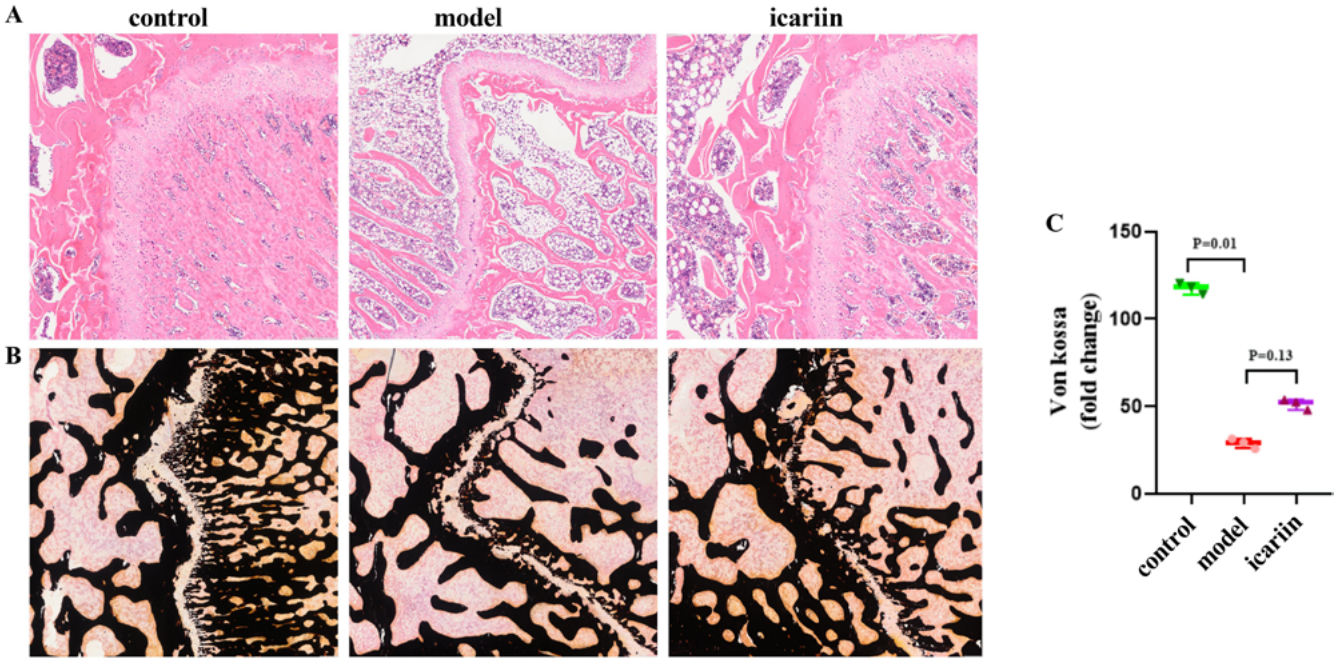

Fig. 3. Icariin restored abnormal morphological structure and calcium levels. A. Hematoxylin and eosin (H&E) staining was used to evaluate the morphological features of the femur (scale bars: 200 μm); B. Calcium nodules were observed using von Kossa staining (scale bars: 200 μm); C. The number of the calcium nodules was quantified in the 3 groups. The Kruskal–Wallis H test indicated significant difference (H = 6.25, p = 0.04). Dunn's post hoc test was performed between group means. Box bodies represent M (p_{25}, p_{27}), upper bars and lower bars represent maximum and minimum, respectively (n = 3). The number of the calcium nodules was reduced in the model group and increased in the icariin group

Table 4. Expression of bone mineral density (BMD) and trabecular parameters in the femur

Index	Group	Index value	95% CI	F value (one-way ANOVA)	p-value	H value	p-value
BMD (X ±S) [g/cm^2]	control	1.12 ±0.15	(0.88, 1.37)	35.07	0.00	–	–
	model	0.35 ±0.17***	(0.08, 0.61)				
	icariin	0.97 ±0.08$^{\#\#\#}$	(0.84, 1.10)				
Bv/Tv (X ±S) (%)	control	73.98 ±6.73	(63.27, 84.68)	56.64	0.00	–	–
	model	9.04 ±1.33***	(6.92, 11.16)				
	icariin	41.37 ±13.28***$^{\#\#\#}$	(20.24, 62.49)				
Bs/Bv (X ±S) [1/mm]	control	19.99 ±3.82	(13.91, 26.07)	32.76	0.00	–	–
	model	39.83 ±1.32***	(37.73, 41.93)				
	icariin	28.03 ±4.49**$^{\#\#\#}$	(20.89, 35.18)				
Tb.Th (X ±S) [mm]	control	0.18 ±0.01	(0.16, 0.19)	33.83	0.00	–	–
	model	0.09 ±0.01***	(0.07, 0.11)				
	icariin	0.13 ±0.02***$^{\#\#}$	(0.09, 0.16)				
Tb.Sp (X ±S) [mm]	control	0.08 ±0.01	(0.07, 0.10)	224.48	0.00	–	–
	model	0.80 ±0.04***	(0.74, 0.86)				
	icariin	0.25 ±0.08***$^{\#\#\#}$	(0.13, 0.38)				
Tb.N, M (p_{25}, p_{75}) [1/mm]	control	4.45 (4.30, 4.80)	–	–	–	8.91	0.01
	model	1.32 (1.00, 1.40)**	–				
	icariin	3.24 (2.90, 3.90)	–				

** p ≤ 0.01 compared to the control group; * p ≤ 0.001 compared to the control group; $^{\#\#}$p ≤ 0.01 compared to the model group; $^{\#\#\#}$p ≤ 0.001 compared to the model group; BMD – bone marrow density; BV/TV – bone volume over total volume; Bs/Bv – bone surface over bone volume; Tb.Th – trabecular thickness; Tb.N – trabecular number; Tb.Sp – trabecular spacing.

The Bv/Tv, Tb.Th, Tb.N, Bs/Bv, and Tb.Sp parameters reflect the morphological trabecula structure. The Bv/Tv, Tb.Th and Tb.N in the model group were found to be lower than in the control group, while Bs/Bv and Tb.Sp were higher. Icariin increased Bv/Tv, Tb.Th and Tb.N and decreased Bs/Bv and Tb.Sp (Table 4).

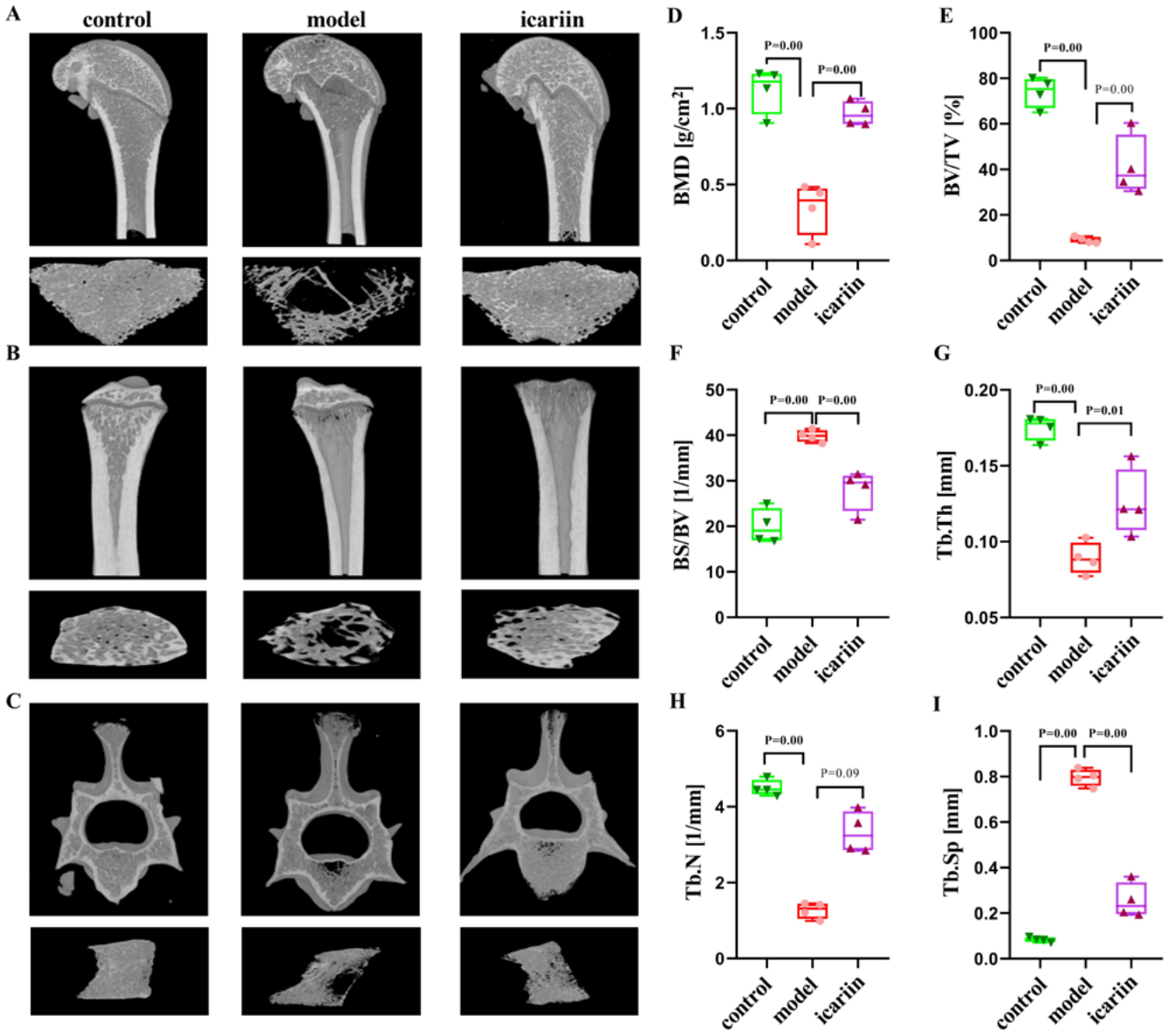

Fig. 4. Icariin adjusted the trabecular state and parameters. A. Trabecular bones in femur; B. Trabecular bones in tibi; C. Trabecular bones in lumbar (L4). A, B and C were scanned using micro-computed tomography (CT); D. Bone mineral density (BMD): quantification of trabecular bone volume and architecture ($F_{2,9} = 35.07$, $p = 0.00$); E. Bone volume over total volume (BV/TV) ($F_{2,9} = 56.64$, $p = 0.00$); F. Bone surface to bone volume (BS/BV) ($F_{2,9} = 32.76$, $p = 0.00$); G. Trabecular thickness (Tb.Th) ($F_{2,9} = 33.83$, $p = 0.00$); H. Trabecular number (Tb. N) ($H = 8.91$) ($p = 0.01$); I. Trabecular spacing (Tb.Sp) ($F_{2,9} = 224.48$, $p = 0.00$). One-way analysis of variance (ANOVA) and least significant difference (LSD) post hoc tests were performed in the D, E, F, G, and I plots. The Kruskal–Wallis H test and Dunn's post hoc test were performed in H plots. Box bodies represent M (p_{25}, p_{75}), and upper bars and lower bars represent maximum and minimum, respectively (n = 4). The BMD, BV/TV, Tb.Th, and Tb.N in the model group were lower than in the control group, while BS/BV and Tb.Sp were higher. Icariin increased BMD, BV/TV, Tb.Th, Tb.N and decreased BS/BV and Tb.Sp

Autophagy of the OP rats activated by icariin

Autophagy-associated proteins were evaluated using western blotting. As shown in Fig. 5, LC3II/LC3I, Atg7 and Beclin1 were decreased, while p62 was increased in the model group compared to the control group. Icariin increased the levels of LC3II/LC3I, Atg7 and Beclin 1, and decreased the expression of p62 compared to the model group (Table 5).

A bidirectional switch effect of icariin on autophagy pathways

The ULK1 is a pivotal modulator of autophagy initiation.[15] The Ser555 and Ser757 phosphorylation sites of ULK1 have distinct effects on autophagy. Phosphorylation at the Ser555 site induces autophagy, while phosphorylation at the Ser757 site inhibits autophagy.[16,17] For the model group, Fig. 6E,F show that ULK1 phosphorylated at Ser555 decreased but ULK1 phosphorylated at Ser757 increased. However, icariin increased Ser555-phosphorylated ULK1 and decreased Ser757-phosphorylated ULK1.

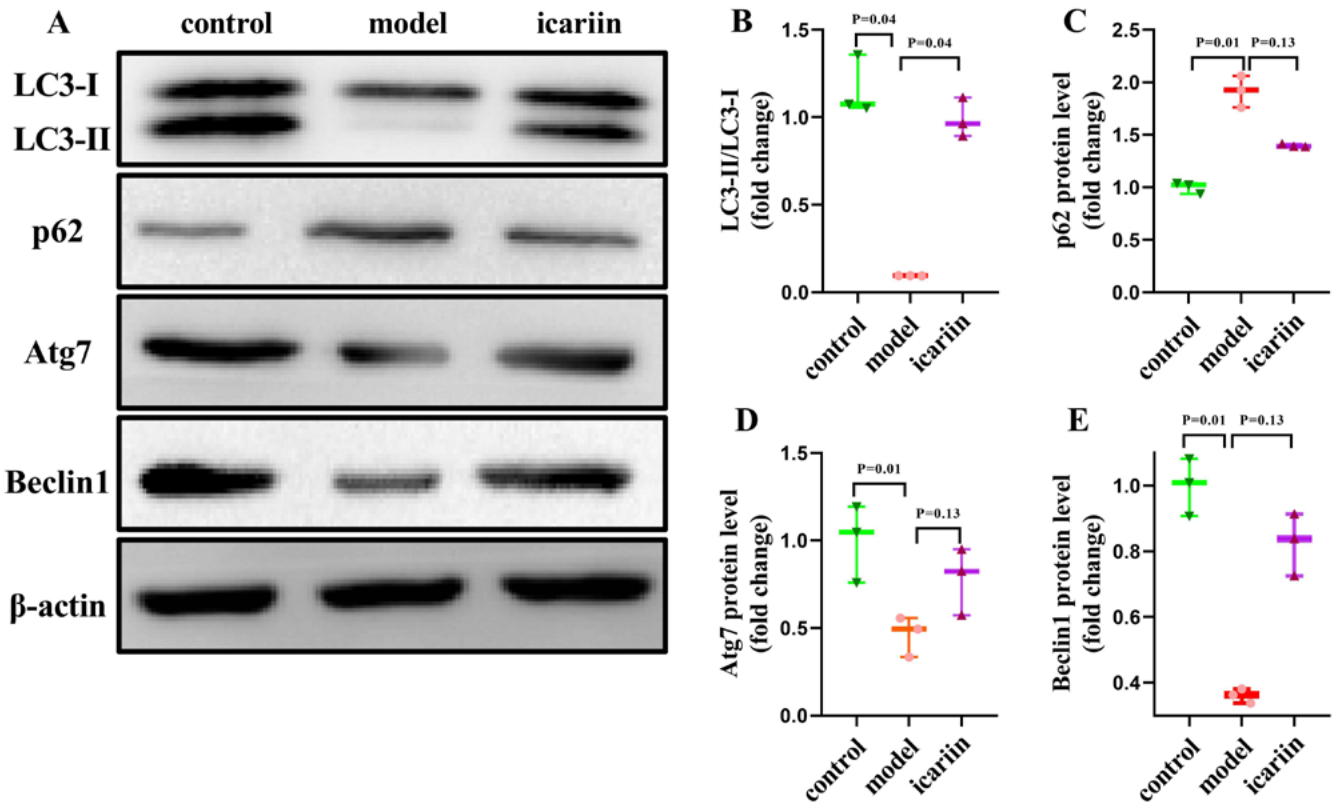

Fig. 5. Icariin activated autophagy levels in osteoporosis (OP) rats. A. Autophagy-associated protein expression of microtubule-associated protein 1 light chain 3 (LC3), sequestosome 1 (p62), autophagy-related protein 7 (Atg7), and Beclin1 in femur by western blotting; B. Quantification of LC3II/LC3I ($H = 6.30$, $p = 0.04$); C. Quantification of p62 ($H = 6.25$, $p = 0.04$); D. Quantification of Atg7 ($H = 6.25$, $p = 0.04$); E. Quantification of Beclin1 ($H = 6.25$, $p = 0.04$). The Kruskal–Wallis H test and Dunn's post hoc test were performed in B, C, D, and E plots. Box bodies represent M (p_{25}, p_{75}), upper bars and lower bars represent maximum and minimum, respectively ($n = 3$). The LC3II/LC3I, Atg7 and Beclin1 were decreased, while p62 was increased in the model group. Icariin increased the level of LC3II/LC3I, Atg7 and Beclin1 and decreased the expression of p62

Table 5. Levels of autophagy proteins in rats (M (p_{25}, p_{75}))

Protein	Group	Gray value	H value	p-value
LC3II/LC3I	control	1.08 (1.05, 1.36)	6.30	0.04
	model	0.10 (0.09, 0.10)*		
	icariin	0.96 (0.89, 1.11)		
Atg7	control	1.05 (0.76, 1.19)	6.25	0.04
	model	0.49 (0.33, 0.56)*		
	icariin	0.82 (0.57, 0.95)		
Beclin1	control	1.01 (0.91, 1.08)	6.25	0.04
	model	0.36 (0.34, 0.38)*		
	icariin	0.84 (0.73, 0.91)		
p62	control	1.02 (0.94, 1.04)	6.25	0.04
	model	1.93 (1.76, 2.06)*		
	icariin	1.39 (1.39, 1.41)		

* $p < 0.05$ compared to the control group.

The Akt and mTOR, as downstream targets, act on the Ser757 phosphorylation site of ULK1 and are negatively associated with autophagy regulation.[18] As shown in Fig. 6A–C, phosphorylation of Akt and mTOR resulted in significant activation in the model group. However, icariin suppressed the change.

Another upstream kinase, AMPK, acts on the kinase at the Ser555 phosphorylation site of ULK1. As shown in Fig. 6A,D, AMPK levels were significantly suppressed in the model group. Icariin elevated AMPK phosphorylation levels.

The results show that OP modelling in rats suppressed the AMPK/ULK1 pathway and activated the Akt/mTOR/

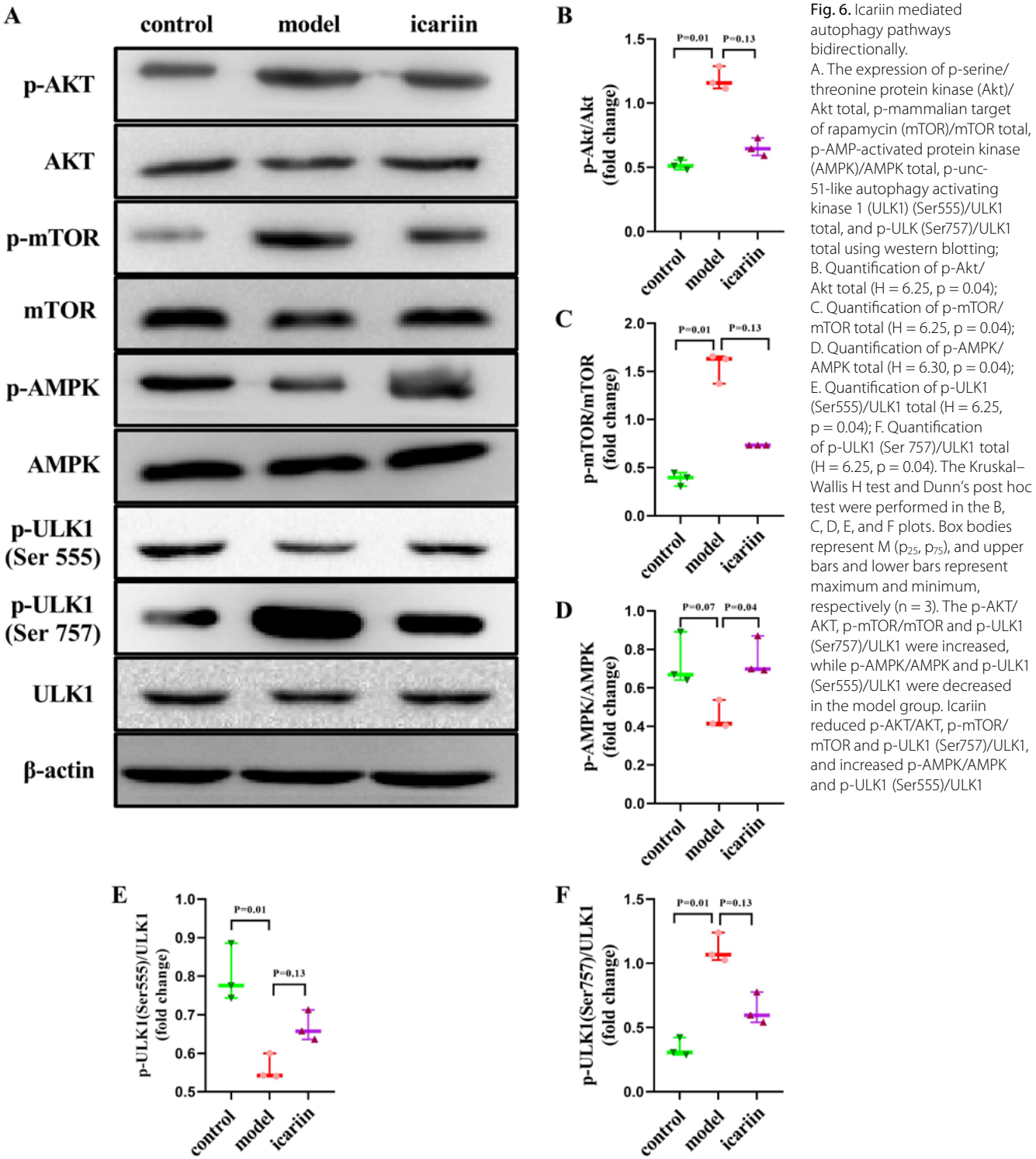

Fig. 6. Icariin mediated autophagy pathways bidirectionally. A. The expression of p-serine/threonine protein kinase (Akt)/Akt total, p-mammalian target of rapamycin (mTOR)/mTOR total, p-AMP-activated protein kinase (AMPK)/AMPK total, p-unc-51-like autophagy activating kinase 1 (ULK1) (Ser555)/ULK1 total, and p-ULK (Ser757)/ULK1 total using western blotting; B. Quantification of p-Akt/Akt total (H = 6.25, p = 0.04); C. Quantification of p-mTOR/mTOR total (H = 6.25, p = 0.04); D. Quantification of p-AMPK/AMPK total (H = 6.30, p = 0.04); E. Quantification of p-ULK1 (Ser555)/ULK1 total (H = 6.25, p = 0.04); F. Quantification of p-ULK1 (Ser 757)/ULK1 total (H = 6.25, p = 0.04). The Kruskal–Wallis H test and Dunn's post hoc test were performed in the B, C, D, E, and F plots. Box bodies represent M (p_{25}, p_{75}), and upper bars and lower bars represent maximum and minimum, respectively (n = 3). The p-AKT/AKT, p-mTOR/mTOR and p-ULK1 (Ser757)/ULK1 were increased, while p-AMPK/AMPK and p-ULK1 (Ser555)/ULK1 were decreased in the model group. Icariin reduced p-AKT/AKT, p-mTOR/mTOR and p-ULK1 (Ser757)/ULK1, and increased p-AMPK/AMPK and p-ULK1 (Ser555)/ULK1

ULK1 pathway, while icariin induced autophagy in a bidirectional switch manner (Table 6).

Discussion

With an aging population, the incidence of OP is a global concern.[19] Serious clinical symptoms such as movement restriction, body deformity, chronic pain, and disability seriously reduce the quality of patients' life, and therefore, an efficient prevention and treatment strategy is urgently required.[20] Osteoporosis is treated clinically with synthetic drugs despite their numerous side effects.[21] Icariin is a natural herbal extract component that exhibits important pharmacological activities for metabolic bone diseases.[22] Autophagy regulates bone balance through bone formation and bone resorption.[9] The present study investigated the potential of icariin in OP treatment and elucidated its possible mechanism of action in autophagy.

Table 6. Expression of autophagy pathways protein in femur (M (p_{25}, p_{75}))

Protein	Group	Odds of gray value	H value	p-value
Ser555/ULK1	control	0.78 (0.74, 0.89)	6.25	0.04
	model	0.54 (0.54, 0.60)*		
	icariin	0.66 (0.64, 0.71)		
Ser757/ULK1	control	0.31 (0.29, 0.42)	6.25	0.04
	model	1.07 (1.03, 1.24)*		
	icariin	0.60 (0.54, 0.78)		
p-Akt/Akt	control	0.51 (0.48, 0.56)	6.25	0.04
	model	1.16 (1.11, 1.29)*		
	icariin	0.64 (0.59, 0.73)		
p-mTOR/mTOR	control	0.40 (0.31, 0.45)	6.56	0.04
	model	1.63 (1.37, 1.66)*		
	icariin	0.73 (0.73, 0.73)		
p-AMPK/AMPK	control	0.67 (0.64, 0.89)	6.30	0.04
	model	0.41 (0.40, 0.54)		
	icariin	0.70 (0.69, 0.87)#		

* $p < 0.05$ compared to the control group; #$p < 0.05$ compared to the model group; ULK1 – unc-51-like autophagy activating kinase 1; Akt – serine/threonine protein kinase; mTOR – mammalian target of rapamycin; AMPK – AMP-activated protein kinase.

The OP rat model was established by ovariectomy, simulating bone mass loss and structural changes due to estrogen deficiency. Icariin intervention counteracted the increased weight, graying of hair, and slowing of reflexes that were observed in the model group, possibly by restoring the endocrine imbalance and slowing lipid metabolism caused by OP. Bones maintain a dynamic balance through osteoblastic formation and osteoclastic resorption. The ALP and PINP in serum are markers of osteoblastic formation, and CTX-I and TRACP-5b are specific markers of bone resorption, which increases in high turnover bone disease.[23–26] The blood serum analysis demonstrated that icariin reduced the indicators of bone formation and resorption, and enhanced bone turnover in rats in vivo. Micro-CT is an innovative method for assessing microstructural changes in bone tissue, which is simple, noninvasive and non-destructive to the specimen. Micro-CT scans revealed that icariin increased BMD and improved the trabecula parameters in the OVX rat model. Calcium nodules are mineralized products of the OBs, which can reflect the OB properties. The von Kossa staining revealed an apparent increase in the number of calcium nodules after icariin treatment compared with the OVX group. Therefore, icariin can promote OB formation and differentiation.

At present, the mechanism and targets for OP are unclear, so there are no particularly effective drugs on the market. In this study, autophagy marker proteins, namely Atg7, LC3II/LC3I, p62, and Beclin 1, were measured. The *Atg7*, an autophagy-related gene, is essential for autophagy, and the Atg system can promote LC3II binding and assist autophagosome elongation and closure. Beclin 1 is a protein involved in vesicle trafficking and autophagosome maturation, and increased expression of p62 can cause protein-specific autophagy degradation.[27] Our study showed that the autophagy activation factors LC3II/LCI, Atg7 and Beclin 1 were reduced while inhibitory factor p62 was increased in OP rats. This situation was reversed after the intervention with icariin. These results confirm other literature precedents indicating that OP is associated with decreased levels of autophagy.[28]

Our research focused on explaining the bidirectional effects of the autophagy AMPK/ULK1 and AKT/mTOR/ULK1 pathways on OP. The ULK1 is the first initiation complex of autophagy.[29] The Ser555 and Ser757 phosphorylation sites of ULK1 have distinct effects on autophagy. The AMPK stimulates the phosphorylation of the ULK1, while AKT and mTOR are inhibitors.[30,31] This paper reveals that, in OP rats, ULK1 protein phosphorylated at the Ser555 phosphorylation decreased, but ULK1 phosphorylated at Ser757 increased. Therefore, impaired autophagy can induce OP, and appropriate activation of autophagy can have a protective effect against OP. The AMPK acted on the kinase at the ULK1 Ser555 phosphorylating site, and the AMPK/ULK1 (Ser555) pathway was suppressed in OP rats in vivo. The mTOR and AKT acted on the ULK1 Ser757 phosphorylating site and the mTOR/AKT/Ulk1 (Ser757) autophagy pathway was promoted. However, the activities of AMPK, AKT, mTOR, ULK1 (Ser757), and ULK1 (Ser555) were modified by the intervention with icariin. The overexpression of AKT, mTOR and ULK1 (Ser757) was suppressed, and low AMPK and ULK1 (Ser555) were improved by icariin. In summary, icariin induced autophagy by activating the AMPK/ULK1 (Ser555) pathway and suppressing the AKT/mTOR/ULK1 pathway.

Icariin affects bone metabolism in various ways. For example, for ULK1, icariin stimulates the osteoblastic differentiation of bone marrow-derived mesenchymal stem cells,

adjusting the bone metabolism balance.[32] This is a separate mechanism. In this study, only 2 signaling pathways, AMPK/ULK1 and Akt/mTOR/ULK1 in the autophagy pathway, were selected for study. In our subsequent experiments, we will consider using mesenchymal stem cells from bone marrow to induce osteogenic differentiation and confirm the in vivo experiments.

Limitations

Our research explained the bidirectional effects of the autophagy AMPK/ULK1 and AKT/mTOR/ULK1 pathways on OP. Meanwhile, the mechanisms of the icariin treatment in OP by its mediation of autophagy were explained. However, our study still has some limitations. This research is too basic for further analysis, and deeper investigations are needed. Particularly, this study should be repeated with the addition of another group (ovariectomy+icariin+autophagy inhibitor) to prove the participation of autophagy in the mechanism. Thus, we were not able to fully confirm the in vivo results. We will further examine the mechanism in vitro.

Conclusions

In conclusion, daily oral administration of icariin for 12 weeks restored femur microstructure and increased bone turnover, effectively impeding bone loss caused by OP in rats. The molecular mechanism, at least partially, involves the regulation of the AMPK/ULK1 and AKT/mTOR/ULK1 autophagy pathways. The results provide an experimental basis for the further development of icariin in the field of OP treatment.

Supplementary data

The Supplementary materials are available at https://doi.org/10.5281/zenodo.8415761). The package consists of the following files:

Supplementary Table 1. Results of normality and variance homogeneity test of body weights at the 12th week (X±S).

Supplementary Table 2. Results of normality and variance homogeneity test of indexes of bone formation and resorption in serum (X ±S).

Supplementary Table 3. Results of normality and variance homogeneity test of BMD and trabecular parameters in femur.

ORCID iDs

Jiaying Zou https://orcid.org/0009-0005-1486-1121
Yue Peng https://orcid.org/0000-0001-6036-3880
Yue Wang https://orcid.org/0009-0008-1241-0767
Shouzhu Xu https://orcid.org/0000-0003-0596-5939
Chuandao Shi https://orcid.org/0000-0002-1434-1100
Qiling Liu https://orcid.org/0000-0002-3479-5601

References

1. Zeng L, Yu G, Yang K, Hao W, Chen H. The improving effect and safety of probiotic supplements on patients with osteoporosis and osteopenia: A systematic review and meta-analysis of 10 randomized controlled trials. *Evid Based Complement Alternat Med*. 2021;2021:9924410. doi:10.1155/2021/9924410
2. Damani JJ, De Souza MJ, VanEvery HL, Strock NCA, Rogers CJ. The role of prunes in modulating inflammatory pathways to improve bone health in postmenopausal women. *Adv Nutr*. 2022;13(5):1476–1492. doi:10.1093/advances/nmab162
3. Surguchov A, Bernal L, Surguchev AA. Phytochemicals as regulators of genes involved in synucleinopathies. *Biomolecules*. 2021;11(5):624. doi:10.3390/biom11050624
4. Mok S, Chen W, Lai W, et al. Icariin protects against bone loss induced by oestrogen deficiency and activates oestrogen receptor-dependent osteoblastic functions in UMR 106 cells. *Br J Pharmacol*. 2010; 159(4):939–949. doi:10.1111/j.1476-5381.2009.00593.x
5. Zu Y, Mu Y, Li Q, Zhang ST, Yan HJ. Icariin alleviates osteoarthritis by inhibiting NLRP3-mediated pyroptosis. *J Orthop Surg Res*. 2019; 14(1):307. doi:10.1186/s13018-019-1307-6
6. Yu T, Xiong Y, Luu S, et al. The shared KEGG pathways between icariin-targeted genes and osteoporosis. *Aging*. 2020;12(9):8191–8201. doi:10.18632/aging.103133
7. Long Z, Wu J, Xiang W, Zeng Z, Yu G, Li J. Exploring the mechanism of icariin in osteoporosis based on a network pharmacology strategy. *Med Sci Monit*. 2020;26:e924699. doi:10.12659/MSM.924699
8. Qi M, Zhang L, Ma Y, et al. Autophagy maintains the function of bone marrow mesenchymal stem cells to prevent estrogen deficiency-induced osteoporosis. *Theranostics*. 2017;7(18):4498–4516. doi:10.7150/thno.17949
9. Yin X, Zhou C, Li J, et al. Autophagy in bone homeostasis and the onset of osteoporosis. *Bone Res*. 2019;7(1):28. doi:10.1038/s41413-019-0058-7
10. Nollet M, Santucci-Darmanin S, Breuil V, et al. Autophagy in osteoblasts is involved in mineralization and bone homeostasis. *Autophagy*. 2014;10(11):1965–1977. doi:10.4161/auto.36182
11. Liu ZZ, Hong CG, Hu WB, et al. Autophagy receptor OPTN (optineurin) regulates mesenchymal stem cell fate and bone–fat balance during aging by clearing FABP3. *Autophagy*. 2021;17(10):2766–2782. doi:10.1080/15548627.2020.1839286
12. Wang S, Deng Z, Ma Y, et al. The role of autophagy and mitophagy in bone metabolic disorders. *Int J Biol Sci*. 2020;16(14):2675–2691. doi:10.7150/ijbs.46627
13. Yoshida G, Kawabata T, Takamatsu H, et al. Degradation of the NOTCH intracellular domain by elevated autophagy in osteoblasts promotes osteoblast differentiation and alleviates osteoporosis. *Autophagy*. 2022;18(10):2323–2332. doi:10.1080/15548627.2021.2017587
14. Liu H, Zhu R, Liu C, et al. Evaluation of decalcification techniques for rat femurs using HE and immunohistochemical staining. *BioMed Res Int*. 2017;2017:9050754. doi:10.1155/2017/9050754
15. Grunwald DS, Otto NM, Park JM, Song D, Kim DH. GABARAPs and LC3s have opposite roles in regulating ULK1 for autophagy induction. *Autophagy*. 2020;16(4):600–614. doi:10.1080/15548627.2019.1632620
16. Wu X, Liu J, Song H, Yang Q, Ying H, Liu Z. Aurora kinase-B silencing promotes apoptosis of osteosarcoma 143B cells by ULK1 phosphorylation-induced autophagy [in Chinese]. *Nan Fang Yi Ke Da Xue Xue Bao*. 2020;40(9):1273–1279. doi:10.12122/j.issn.1673-4254.2020.09.08
17. Liu HT, Pan SS. Late exercise preconditioning promotes autophagy against exhaustive exercise-induced myocardial injury through the activation of the AMPK-mTOR-ULK1 pathway. *BioMed Res Int*. 2019;2019:5697380. doi:10.1155/2019/5697380
18. Walker CL, Walker MJ, Liu NK, et al. Systemic bisperoxovanadium activates Akt/mTOR, reduces autophagy, and enhances recovery following cervical spinal cord injury. *PLoS One*. 2012;7(1):e30012. doi:10.1371/journal.pone.0030012
19. Tanha K, Fahimfar N, Nematollahi S, et al. Annual incidence of osteoporotic hip fractures in Iran: A systematic review and meta-analysis. *BMC Geriatr*. 2021;21(1):668. doi:10.1186/s12877-021-02603-1
20. Yong E, Logan S. Menopausal osteoporosis: Screening, prevention and treatment. *Singapore Med J*. 2021;62(4):159–166. doi:10.11622/smedj.2021036

21. Wang T, Liu Q, Tjhioe W, et al. Therapeutic potential and outlook of alternative medicine for osteoporosis. *Curr Drug Targets*. 2017;18(9). doi:10.2174/1389450118666170321105425
22. Zhang X, Chen Y, Zhang C, et al. Effects of icariin on the fracture healing in young and old rats and its mechanism. *Pharm Biol*. 2021; 59(1):1243–1253. doi:10.1080/13880209.2021.1972121
23. Gillet M, Vasikaran S, Inderjeeth C. The role of PINP in diagnosis and management of metabolic bone disease. *Clin Biochem Rev*. 2021; 42(1):3–10. doi:10.33176/AACB-20-0001
24. Sharma U, Pal D, Prasad R. Alkaline phosphatase: An overview. *Indian J Clin Biochem*. 2014;29(3):269–278. doi:10.1007/s12291-013-0408-y
25. Abe S, Yoshihisa A, Ichijo Y, et al. Serum TRACP5b, a marker of bone resorption, is associated with adverse cardiac prognosis in hospitalized patients with heart failure. *CJC Open*. 2021;3(4):470–478. doi:10.1016 /j.cjco.2020.12.005
26. Bauer D, Krege J, Lane N, et al. National Bone Health Alliance Bone Turnover Marker Project: Current practices and the need for US harmonization, standardization, and common reference ranges. *Osteoporos Int*. 2012;23(10):2425–2433. doi:10.1007/s00198-012-2049-z
27. Florencio-Silva R, Sasso GRDS, Simões MDJ, et al. Osteoporosis and autophagy: What is the relationship? *Rev Assoc Med Bras*. 2017;63(2): 173–179. doi:10.1590/1806-9282.63.02.173
28. Camuzard O, Santucci-Darmanin S, Breuil V, et al. Sex-specific autophagy modulation in osteoblastic lineage: A critical function to counteract bone loss in female. *Oncotarget*. 2016;7(41):66416–66428. doi:10.18632/oncotarget.12013
29. Zachari M, Ganley IG. The mammalian ULK1 complex and autophagy initiation. *Essays Biochem*. 2017;61(6):585–596. doi:10.1042/EBC 20170021
30. Kim J, Kundu M, Viollet B, Guan KL. AMPK and mTOR regulate autophagy through direct phosphorylation of Ulk1. *Nat Cell Biol*. 2011;13(2): 132–141. doi:10.1038/ncb2152
31. Xiang H, Zhang J, Lin C, Zhang L, Liu B, Ouyang L. Targeting autophagy-related protein kinases for potential therapeutic purpose. *Acta Pharm Sin B*. 2020;10(4):569–581. doi:10.1016/j.apsb.2019.10.003
32. Wang Z, Wang D, Yang D, Zhen W, Zhang J, Peng S. The effect of icariin on bone metabolism and its potential clinical application. *Osteoporos Int*. 2018;29(3):535–544. doi:10.1007/s00198-017-4255-1